A mouse model of pseudohypoaldosteronism type II reveals a novel mechanism of renal tubular acidosis

Karen López-Cayuqueo, Maria Chavez-Canales, Alexia Pillot, Pascal Houillier, Maximilien Jayat, Jennifer Baraka-Vidot, Francesco Trepiccione, Véronique Baudrie, Cara Büsst, Christelle Soukaseum, et al.

A mouse model of pseudohypoaldosteronism type II reveals a novel mechanism of renal tubular acidosis

see commentary on page 457

Karen I. López-Cayuqueo[1,2,8], Maria Chavez-Canales[1,8], Alexia Pillot[3], Pascal Houillier[3,4], Maximilien Jayat[1], Jennifer Baraka-Vidot[6], Francesco Trepiccione[1,10], Véronique Baudrie[1,4], Cara Büsst[1,11], Christelle Soukaseum[1], Yusuke Kumai[1], Xavier Jeunemaître[1,4], Juliette Hadchouel[1], Dominique Eladari[1,5,6,9] and Régine Chambrey[1,6,7,9]

[1]*Institut National de la Santé et de la Recherche Médicale, Unité Mixte de Recherche 970, Paris, France;* [2]*Centro de Estudios Científicos, Valdivia, Chile;* [3]*Centre National de la Recherche Scientifique Equipe de Recherche Labelisée 8228, Institut National de la Santé et de la Recherche Médicale, Unité Mixte de Recherche_S1138, Centre de Recherche des Cordeliers, Paris, France;* [4]*Genetics, Assistance Publique-Hôpitaux de Paris, Hôpital Européen Georges Pompidou, Paris, France;* [5]*Service d'Explorations Fonctionnelles Rénales, Hôpital Felix Guyon, CHU de la Réunion, Saint Denis, La Réunion, France;* [6]*Institut National de la Santé et de la Recherche Médicale, Unité Mixte de Recherche 1188, CYROI, Sainte Clotilde, La Réunion, France; and* [7]*Centre National de la Recherche Scientifique, Délégation Paris Michel-Ange, Paris, France*

Pseudohypoaldosteronism type II (PHAII) is a genetic disease characterized by association of hyperkalemia, hyperchloremic metabolic acidosis, hypertension, low renin, and high sensitivity to thiazide diuretics. It is caused by mutations in the *WNK1*, *WNK4*, *KLHL3* or *CUL3* gene. There is strong evidence that excessive sodium chloride reabsorption by the sodium chloride cotransporter NCC in the distal convoluted tubule is involved. WNK4 is expressed not only in distal convoluted tubule cells but also in β−intercalated cells of the cortical collecting duct. These latter cells exchange intracellular bicarbonate for external chloride through pendrin, and therefore, account for renal base excretion. However, these cells can also mediate thiazide-sensitive sodium chloride absorption when the pendrin-dependent apical chloride influx is coupled to apical sodium influx by the sodium-driven chloride/bicarbonate exchanger. Here we determine whether this system is involved in the pathogenesis of PHAII. Renal pendrin activity was markedly increased in a mouse model carrying a WNK4 missense mutation (Q562E) previously identified in patients with PHAII. The upregulation of pendrin led to an increase in thiazide-sensitive sodium chloride absorption by the cortical collecting duct, and it caused metabolic acidosis. The function of apical potassium channels was altered in this model, and hyperkalemia was fully corrected by pendrin genetic ablation. Thus, we demonstrate an important contribution of pendrin in renal regulation of sodium chloride, potassium and acid-base homeostasis and in the pathophysiology of PHAII. Furthermore, we identify renal distal bicarbonate secretion as a novel mechanism of renal tubular acidosis.

Kidney International (2018) **94,** 514–523; https://doi.org/10.1016/j.kint.2018.05.001

KEYWORDS: familial hyperkalemic hypertension; Gordon syndrome; hypertension; intercalated cells; pendrin; renal tubular acidosis

Pseudohypoaldosteronism type II (PHAII), also known as Gordon syndrome or familial hyperkalemic hypertension, is a rare genetic disease characterized by the association of hypertension, hyperchloremic metabolic acidosis, and hyperkalemia in the absence of renal failure.[1] The pathogenesis of this syndrome has remained puzzling for decades because hyperkalemia along with renal metabolic acidosis are 2 features of hypoaldosteronism, whereas volume-dependent hypertension is observed in states caused by an excess of mineralocorticoids. A study by Schambelan *et al.* suggests that the disease is caused by excessive electroneutral absorption of chloride by the distal nephron.[2] The observation that most symptoms of PHAII can be corrected by thiazide diuretics supports the possibility that a gain of function of the thiazide-sensitive sodium chloride (NaCl) cotransporter NCC of the distal convoluted tubule (DCT) plays a central role in PHAII. A breakthrough in our understanding of this disease came in 2001 from the discovery that mutations in genes encoding 2 serine-threonine kinases of the WNK family, WNK1 and WNK4, account for PHAII

Correspondence: *Régine Chambrey, INSERM 1188, CYROI, 2 rue Maxime Rivière, 97490 Sainte Clotilde, La Réunion, France. E-mail: regine.chambrey@inserm.fr; or Dominique Eladari, Service d'Explorations Fonctionnelles Rénales, Hôpital Felix Guyon, CHU de la Réunion, Allée des Topazes, CS 11021 - Saint Denis F-97400, La Réunion, France. E-mail: dominique.eladari@inserm.fr*

[8]These authors share first authorship.

[9]These authors share senior authorship.

[10]Current affiliation: Department of Cardio-Thoracic and Respiratory Science, Second University of Naples, Naples, Italy.

[11]Current affiliation: VicHealth, Melbourne, Australia.

Received 13 March 2018; revised 26 April 2018; accepted 3 May 2018; published online 7 July 2018

in some patients.[3] WNK1 and WNK4 are elements of a complex signaling network involved in the regulation of ion transport in the distal nephron.[4] PHAII mutations in the *WNK1* gene are large intronic deletions that cause an increase in WNK1 expression, whereas *WNK4* mutations are missense mutations clustered in a short acidic segment distal to the kinase domain.[3] These missense mutations also result in increased expression of WNK4 due to a decrease in degradation of the protein.[5] The ubiquitin-ligase complex formed by the proteins KLHL3 and CUL3 has been identified as responsible for this degradation,[4] and mutations in both proteins have been recently identified in patients with PHAII.[6,7]

Logically, the studies conducted over the past 15 years have focused on the regulation of NCC by WNK1 and WNK4. Transgenic mice expressing a *WNK4* transgene carrying 1 of the missense mutations identified in PHAII patients (*WNK4*-Q562E; Tg*Wnk4*^{PHAII} mice) displayed all clinical features of the syndrome.[8] The same phenotypes were seen in a *Wnk4*(D561A/+) knock-in mouse model[9] and in *Wnk1*$^{+/FHHt}$ mice, another PHAII model in which the first intron of *Wnk1* is deleted.[10] In these models, increased NCC phosphorylation and expression at the apical cell membrane result in enhanced NaCl absorption by the DCT, and vascular volume expansion, favoring the onset of hypertension. Conversely, *Wnk4* knockout mice exhibited a mild Gitelman-like syndrome, with normal blood pressure, increased plasma renin activity, and reduced NCC expression and phosphorylation.[11]

The aforementioned studies confirm the importance of NCC in the pathogenesis of PHAII syndrome. However, other studies have suggested that increased NCC activity or abundance is not sufficient to cause PHAII. In transgenic mice overexpressing NCC, NCC abundance was increased but the mice displayed a phenotype similar to wild-type mice.[12] Additionally, mice inactivated for KS-WNK1 or Nedd4-2 did not exhibit hyperkalemic hypertension despite increased NCC expression and phosphorylation.[13,14]

In the kidney, WNK4 is expressed not only in the DCT, but has also been found in the cortical collecting duct (CCD).[3,15,16] Alongside the amiloride-sensitive epithelial sodium channel ENaC, which is expressed by principal cells, we have demonstrated the presence of a novel thiazide-sensitive electroneutral NaCl uptake mechanism in renal intercalated cells (ICs) of the CCD.[17] NaCl is taken up from urine by the coordinated action of the Cl^-/HCO_3^- exchanger pendrin/SLC26A4 and the sodium ion (Na^+)-driven $Cl^-/2HCO_3^-$ exchanger NDCBE/SLC4A8. Overexpression of pendrin in ICs can favor the onset of chloride-dependent hypertension, indicating that this system likely plays a role in the regulation of blood pressure *in vivo*.[18] Conversely, pendrin-deficient mice are protected against mineralocorticoid-induced hypertension[19] and develop a lower blood pressure during NaCl restriction.[20] Importantly, acute inactivation of pendrin results in a lower blood pressure.[21] Finally, we demonstrated that NCC compensated for NDCBE inactivation and that double deletion of these proteins in mouse induces hypokalemia.[22] Therefore, we hypothesized that this novel system might be involved in the pathogenesis of PHAII.

In the present study, we demonstrate that PHAII-causing mutation of WNK4 increases pendrin activity and pendrin/NDCBE-dependent NaCl absorption. We also demonstrate that pendrin hyperactivity is necessary to drive hyperchloremic metabolic acidosis and hyperkalemia in PHAII because both symptoms are corrected by pendrin genetic ablation.

RESULTS

Tg*Wnk4*^{PHAII} mice exhibit hyperkalemic metabolic acidosis

As shown in Figure 1a–e, Tg*Wnk4*^{PHAII} mice exhibit the phenotypic abnormalities characteristic of PHAII: metabolic hyperchloremic acidosis and hyperkalemia. Urinary aldosterone excretion was significantly increased in Tg*Wnk4*^{PHAII} mice (Figure 1f), whereas renin mRNA abundance was lower in the PHAII mice (Figure 1g) as observed in most patients experiencing PHAII. As shown by others,[8,9] NCC and phosphor-T53 NCC protein abundance was dramatically increased in Tg*Wnk4*^{PHAII} mice (Figure 1h).

Electroneutral thiazide-sensitive NaCl transport is activated in the CCD of Tg*Wnk4*^{PHAII} mice

Transepithelial fluxes of Na^+ (J_{Na}), potassium ion (K^+; J_K), chloride ion (Cl^-; J_{Cl}) and the transepithelial voltage (V_{te}) were measured in microperfused CCDs isolated from Tg*Wnk4*^{PHAII} mice fed a standard diet (Figure 2). No transport activity was detectable in CCDs isolated from control mice, as previously described.[17] However, CCDs isolated from Tg*Wnk4*^{PHAII} mice exhibited net NaCl absorption but did not develop a significant lumen negative V_{te} and did not secrete K^+, suggesting the absence of detectable ENaC activity. Furthermore, NaCl absorption was fully inhibited by luminal addition of 100 μM hydrochlorothiazide (HCTZ).

Taken together, these experiments demonstrate that electroneutral NaCl transport mediated by pendrin/NDCBE is stimulated by PHAII-causing mutation of WNK4.

ENaC-dependent K^+ transport mechanisms are impaired in Tg*Wnk4*^{PHAII} mice despite unchanged renal ENaC activity

ENaC activity is generally detectable not in the CCD but only in the connecting tubule (CNT), a nephron segment, which is not suitable for *in vitro* microperfusion. Thus, to estimate the total ENaC activity, we next measured the effect of an acute amiloride injection in Tg*Wnk4*^{PHAII} and control mice on urinary Na^+ and K^+ excretion. The natriuretic response to amiloride was identical for both groups (Figure 3a, left panel), suggesting that Na^+ reabsorption through ENaC is not altered in Tg*Wnk4*^{PHAII} mice. However, amiloride had significantly less effect on urinary K^+ excretion in Tg*Wnk4*^{PHAII} mice than in controls (Figure 3a, right panel). These experiments demonstrate that ENaC-dependent K^+ transport mechanisms *per se* are inhibited in Tg*Wnk4*^{PHAII} mice.

We next examined the relative protein abundance of the α and γ subunits of ENaC in *TgWnk4*^{PHAII} and control mice by

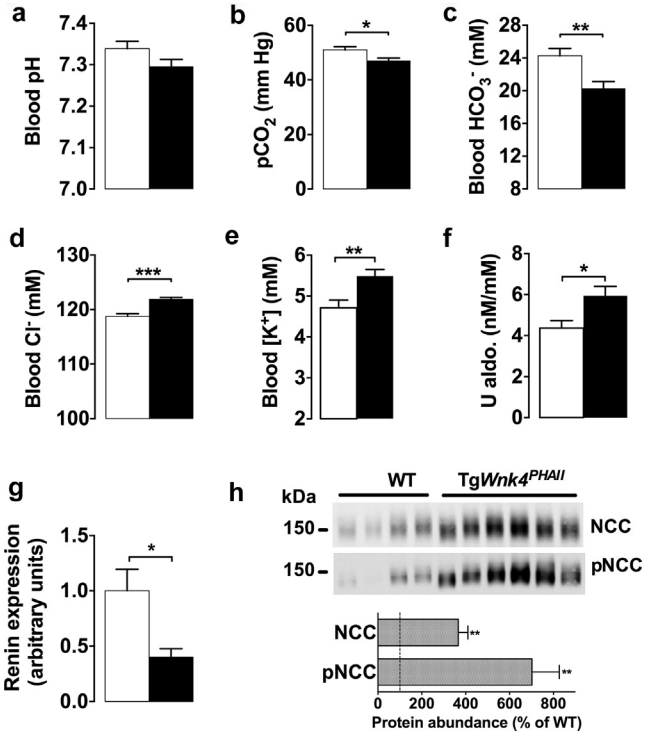

Figure 1 | Tg*Wnk4*^{PHAII} mice exhibit phenotypic abnormalities characteristic of PHAII. (**a–e**) Blood gas and electrolytes were measured in wild-type (white bars) and Tg*Wnk4*^{PHAII} (black bars) mice. Values are represented as mean ± SEM, $n = 8$ mice per group. Statistical significance was assessed by unpaired Student *t*-test. *$P <$ 0.05, **$P < 0.01$, and ***$P < 0.001$. (**f**) Urinary aldosterone (U aldo.) excretion was measured in wild-type (white bars) and Tg*Wnk4*^{PHAII} (black bars) mice. Data are presented as mean ± SEM, $n = 8$ for control mice and $n = 7$ for Tg*Wnk4*^{PHAII} mice. Statistical significance was assessed by unpaired Student *t*-test. *$P < 0.05$. (**g**) Renin gene expression was analyzed by quantitative reverse-transcription polymerase chain reaction in whole kidney of wild-type (white bars) and Tg*Wnk4*^{PHAII} (black bars) mice. Results are expressed in arbitrary units relative to the expression of a geometrical mean of 4 housekeeping genes: ubiquitin, HPRT, 18s rRNA, and GAPDH. The control group has been arbitrarily set to 1. Values are represented as mean ± SEM, $n = 6$ mice per group. Statistical significance was assessed by unpaired Student *t*-test. *$P < 0.05$. (**h**) Immunoblots for sodium chloride cotransporter (NCC) and its T53 phosphorylated residue (pNCC) on plasma membrane-enriched fractions from renal cortex of Tg*Wnk4*^{PHAII} ($n = 6$) and wild-type ($n = 4$) mice. Bar graph shows a summary of densitometric analyses. Densitometric values were normalized to the mean for the control group that was defined as 100% and results were expressed as mean ± SEM. Statistical significance was assessed by unpaired Student *t*-test. **$P < 0.001$. To optimize viewing of this image, please see the online version of this article at www.kidney-international.org.

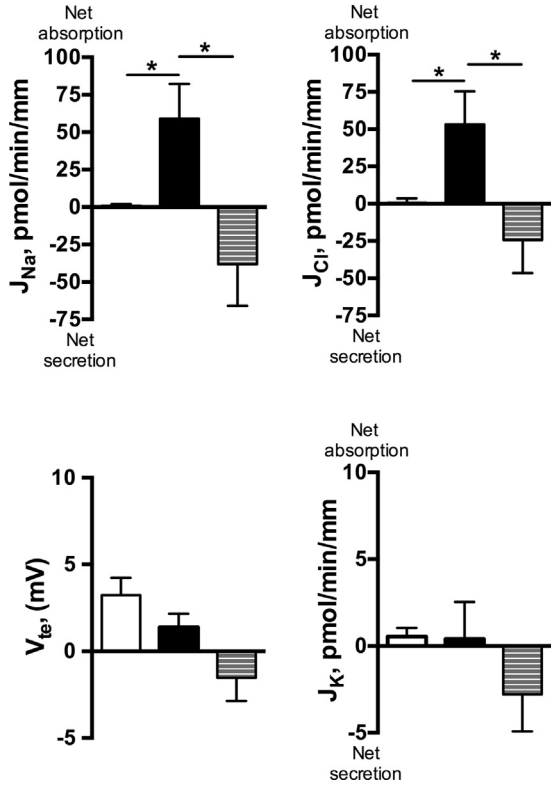

Figure 2 | Electroneutral sodium chloride transport system is activated in the cortical collecting duct (CCD) of Tg*Wnk4*^{PHAII} mice and abolished by luminal HCTZ. Na^+ (JNa), Cl^- (JCl), and K^+(JK) transepithelial fluxes and transepithelial voltage (Vte) were measured in microperfused CCDs isolated from wild-type mice (white bars, $N = 6$) and Tg*Wnk4*^{PHAII} mice (black bars, $N = 5$) fed a standard 0.3% sodium diet. Transepithelial ion fluxes and voltage were also measured in the presence of 100 μM hydrochlorothiazide in the tubular lumen of CCDs isolated from Tg*Wnk4*^{PHAII} mice (striped bars, $N = 6$). Statistical significance was assessed by an unpaired Student *t*-test. *$P < 0.05$.

immunoblot analyses of plasma membrane-enriched preparations isolated from renal cortex (Figure 3b). The abundance of the full-length 90 kDa form and the cleaved N-terminal 30 kDa fragment of α-ENaC was higher in Tg*Wnk4*^{PHAII} mice. The abundance of the full-length form of γ-ENaC (85 kDa) was decreased in Tg*Wnk4*^{PHAII} mice, whereas the abundance of the cleaved 70 kDa form of γ-ENaC was increased. These alterations are indicative of an activation of ENaC possibly by aldosterone.

Normalization of plasma K concentration does not correct metabolic acidosis in Tg*Wnk4*^{PHAII} mice

Hyperkalemia can cause renal tubular acidosis.[23] To check the importance of high plasma potassium in the development of acidosis in PHAII, we tested whether normalization of plasma potassium concentration can alleviate the acidosis of Tg*Wnk4*^{PHAII} *mice*. Tg*Wnk4*^{PHAII} mice were fed with a synthetic low-K^+ diet for 4 days (Figure 4). As expected, plasma K^+ was normalized following this treatment. However, the decrease in plasma K^+ did not modify either plasma HCO_3^- or pH, indicating that acidosis in PHAII is not caused primarily by hyperkalemia.

Renal acidosis in Tg*Wnk4*^{PHAII} mice is not caused by impaired proton secretion

We next evaluated whether metabolic acidosis in Tg*Wnk4*^{PHAII} mice is due to impaired proton secretion by the distal nephron. Acid was administrated as NH_4Cl 0.28 M in the drinking water for 15 days. Figure 5 shows that before acid loading, only plasma HCO_3– (panel b) was significantly lower

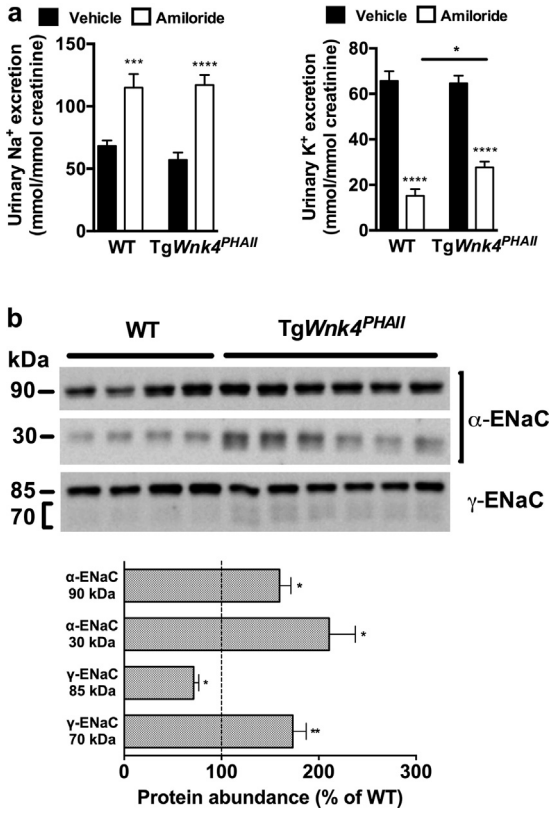

Figure 3 | Epithelial sodium channel (ENaC) expression and activity in Tg*Wnk4*^{PHAII} mice. (**a**) Effect of amiloride injection on urinary Na^+ and K^+ excretion in wild-type and Tg*Wnk4*^{PHAII} mice. Amiloride elicits significant increase in Na^+ excretion and decrease in potassium ion (K^+) excretion in both wild-type and Tg*Wnk4*^{PHAII} mice 6 hours after injection. Amiloride-induced natriuresis was not different between groups. K^+ excretion after amiloride was significantly higher in Tg*Wnk4*^{PHAII} mice, indicating that ENaC-dependent K^+ secretion is decreased in these mice. Values are the mean ± SEM for 8 mice. Statistical significance was assessed by 1-way analysis of variance. ***$P < 0.001$ and ****$P < 0.0001$, vehicle versus amiloride. *$P < 0.05$, wild-type versus Tg*Wnk4*^{PHAII} mice following amiloride injection. (**b**) α-ENaC and γ-ENaC protein abundance was assessed by Western blot of plasma membrane–enriched preparations obtained from the renal cortex of wild-type ($n = 4$) and Tg*Wnk4*^{PHAII} ($n = 6$) mice. Bar graph shows a summary of densitometric analyses. Densitometric values were normalized to the mean for the control group that was defined as 100%, and results were expressed as mean ± SEM. Statistical significance was assessed by unpaired *t*-test. *$P <$ 0.05, **$P < 0.01$. To optimize viewing of this image, please see the online version of this article at www.kidney-international.org.

in Tg*Wnk4*^{PHAII} mice, whereas urine pH (panel c), urinary titrable acid excretion (panel d), and ammonium excretion (panel e) were identical in Tg*Wnk4*^{PHAII} and control mice. After 2 days of acid loading, blood pH and HCO_3– decreased in both groups. However, Tg*Wnk4*^{PHAII} mice developed a much stronger metabolic acidosis. When acid loading was continued, control mice were able to cope with the acid load and exhibited normal blood pH and HCO_3– at day 15 of the treatment. By contrast, severe metabolic acidosis persisted in Tg*Wnk4*^{PHAII} mice. Interestingly, following acid loading, urine pH decreased and ammonium excretion increased maximally in both groups, indicating that proton secretion, and ammonium transport or metabolism, are normal in these mice.

The effect of acid loading was also tested in *WNK1*$^{+/FHHt}$ mice, another PHAII model in which the first intron of *WNK1* is deleted.[10] When submitted to an acid load (Supplementary Figure S1), these mice responded exactly like Tg*Wnk4*^{PHAII} mice, indicating that the same mechanism is causing acidosis in both PHAII models independently of the mutation.

Finally, Figure 5f shows a marked shift in the relationship between urinary ammonium excretion and blood bicarbonate concentration (reflecting the severity of metabolic acidosis) in Tg*Wnk4*^{PHAII} versus control mice. This demonstrated that, while proton secretion or ammonium excretion capabilities are preserved in Tg*Wnk4*^{PHAII} mice, these mice clearly have a defect in renal net acid excretion. This led us to hypothesize that metabolic acidosis in PHAII is not caused by impaired acid excretion but rather is due to increased renal loss of base.

Pendrin activity is increased in PHAII-mutant WNK4 mice

We next examined pendrin activity by measuring Cl^--dependent alkalinization in ICs in CCDs isolated from Tg*Wnk4*^{PHAII} and control mice (Figure 5g, left panel). The rate of intracellular alkalinization in response to luminal Cl^- removal, an estimate of apical Cl^-/HCO_3^- exchange activity, was much higher in ICs from Tg*Wnk4*^{PHAII} mice than in control mice (Figure 5g, right panel). These results indicate that pendrin activity per cell is increased in this model.

Further, immunofluorescence staining revealed an increase in pendrin labeling in the collecting ducts located in renal medullary rays of Tg*Wnk4*^{PHAII} mice (Figure 5h). ICs exist in 3 different forms: (i) α-ICs characterized by apical expression of the V-ATPase and basolateral expression of an anion exchanger, which is an alternately spliced product of the erythrocyte AE1 gene, (ii) β-ICs, which harbor apical pendrin and basolateral V-ATPase, and (iii) non-α-, non-β-ICs with apical pendrin and apical V-ATPase. The total number of ICs remains generally constant; however, the relative number of α-ICs versus β-ICs is tightly controlled and adapted depending on the acid-base status.[24] We therefore evaluated the number of the different versions of ICs in the CCDs of control and Tg*Wnk4*^{PHAII} mice using triple immunofluorescence labeling for pendrin, for the E subunit of the V-ATPase, and for AE1 (Figure 5h). In both transgenic and control mice, CCDs located in medullary rays exhibited α- and β-ICs but no non-α-, non-β-ICs. We counted 1867 ICs (defined as those that stained for the E subunit of the V-ATPase) from 4 independent control mice, and the results are displayed as white bars in Figure 5i. Of these ICs, 37% stained for pendrin, whereas 63% had AE1 staining. In 4 independent Tg*Wnk4*^{PHAII} mice, we counted 1955 ICs (black bars in Figure 5i). The fraction of β-ICs was significantly increased in CCDs of *TgWnk4*^{PHAII} mice as 50% of ICs were pendrin-positive. Conversely, the number of α-ICs was reduced and the total number of ICs was not different

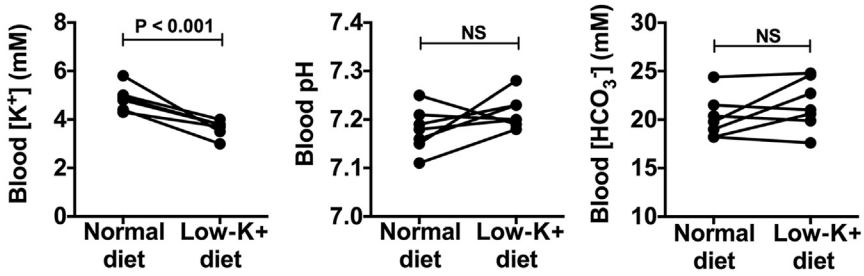

Figure 4 | Low-potassium ion (K+) diet decreases blood plasma potassium concentration in Tg*Wnk4*^{PHAII} mice but does not modify blood pH or blood HCO_3^-. Blood gas parameters were measured in 7 Tg*Wnk4*^{PHAII} mice fed a normal diet and after 4 days on a low-K^+ diet. Statistical analysis was assessed by paired *t*-student. NS, not significant; $P > 0.05$.

between control and Tg*Wnk4*^{PHAII} mice. Because pendrin activity per cell is increased, we can conclude that total pendrin activity is increased in CCDs of mutant mice. As shown in Figure 5j, this increased pendrin transport activity was associated with a significant increase in CCD fractional volume.

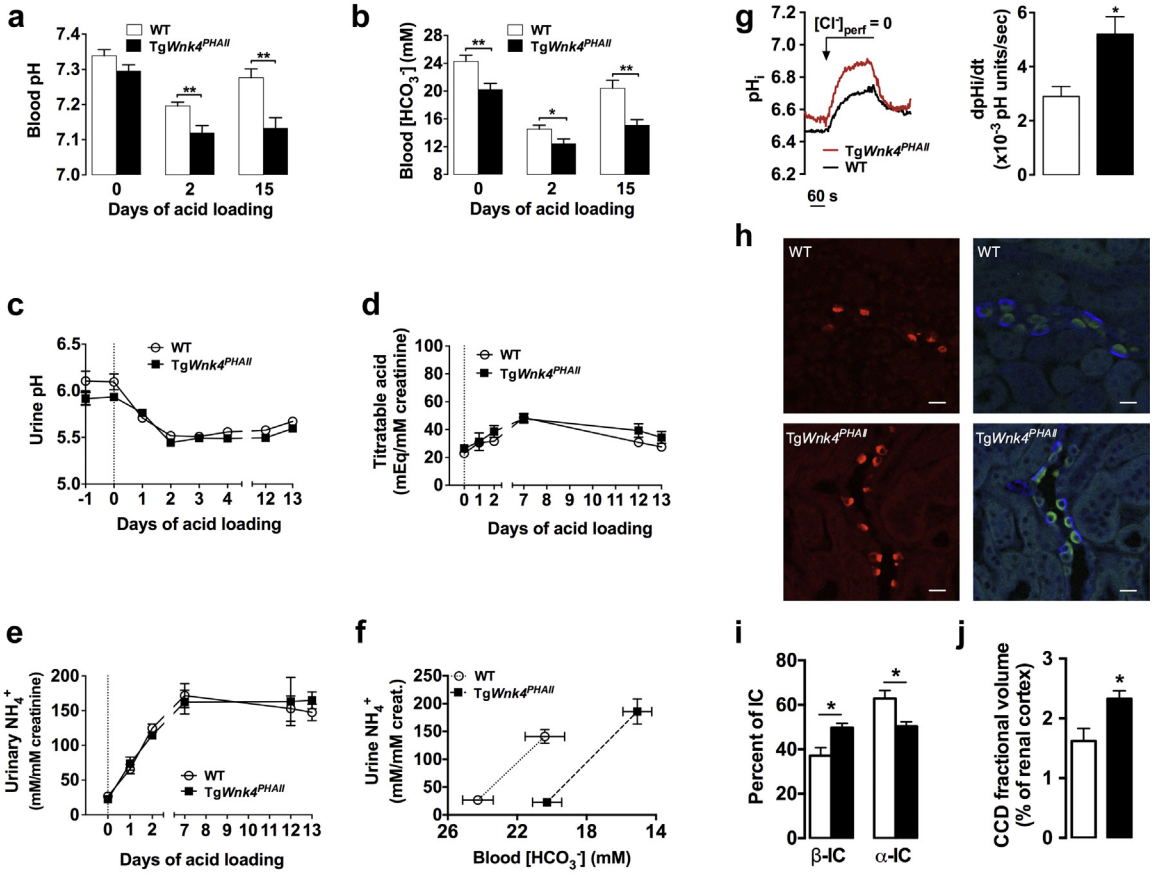

Figure 5 | Tg*Wnk4*^{PHAII} mice display renal tubular acidosis due to increased apical Cl/HCO_3 exchange activity in β-intercalated cells. (**a–e**) Time course of blood gas analysis and urinary acid-base parameters from wild-type (WT; white bar and open circle) and Tg*Wnk4*^{PHAII} mice (black bar and black square) during 15 days of acid loading (280 mM of NH_4Cl in drinking water). Values are represented as the mean ± SEM for 8 mice. Statistical significance was assessed by unpaired Student *t*-test. $^*P < 0.05$, $^{**}P < 0.01$). (**f**) Relationship between urinary NH_4^+ and plasma [HCO_3^-] before and after the acid loading. (**g**) Representative profile of intracellular pH changes following luminal chloride removal in intercalated cells in isolated cortical collecting duct (CCDs) from WT (black curve) and Tg*Wnk4*^{PHAII} (red curve) mice. Average initial rates of pH increase after chloride removal in intercalated cell (ICs) from WT (open bars, $N = 4$) and Tg*Wnk4*^{PHAII} (black bars, $N = 7$) mice. Values are represented as the mean ± SEM, $^*P < 0.05$, unpaired Student *t*-test. (**h**) Immunofluorescence images of collecting ducts in medullary rays from WT and Tg*Wnk4*^{PHAII} mice. Kidney sections were labeled for pendrin, for the E subunit of the V-ATPase, and for AE1. β-ICs were identified as apical pendrin (red) and basolateral V-ATPase (green) positive cells. α-ICs were identified as apical V-ATPase (green) and basolateral AE1 (blue) positive cells. Bar = 50 μm. (**i**) Fraction of α-IC cells and β-IC cells in relation of total ICs in CCD. WT mice (open bars) and Tg*Wnk4*^{PHAII} (black bars), $N = 4$ for each group. $^*P < 0.05$, unpaired *t*-test. (**j**) Fractional volume of CCDs in WT (open bars) and Tg*Wnk4*^{PHAII} mice (black bars), $N = 4$ mice per group. $^*P < 0.05$, unpaired Student *t*-test. To optimize viewing of this image, please see the online version of this article at www.kidney-international.org.

Hyperchloremic metabolic acidosis and hyperkalemia in Tg*Wnk4*^{PHAII} mice are corrected by pendrin genetic ablation

To verify whether hyperactivity of pendrin participates to PHAII phenotype, we next tested the effects of pendrin disruption in mice harboring the mutation of WNK4 causing PHAII. Double-mutant mice (Tg*Wnk4*^{PHAII};*Pds*$^{-/-}$) no longer exhibited hyperchloremic metabolic acidosis and hyperkalemia (Table 1). These results confirmed that activation of pendrin participates to hyperchloremic acidosis and hyperkalemia in PHAII.

Pendrin disruption in Tg*Wnk4*^{PHAII} mice led to a significant increase in hematocrit (Table 1). Renin mRNA was also higher in double transgenic Tg*Wnk4*^{PHAII};*Pds*$^{-/-}$ mice (Figure 6). No significant difference, however, was detected in blood pressure measured by telemetry (Figure 6) or in aldosterone levels (7.26 ± 0.57 nM/mM creatinine in Tg*Wnk4*^{PHAII};*Pds*$^{-/-}$ mice, $n = 10$ vs. 7.93 ± 0.63 nM/mM creatinine in Tg*Wnk4*^{PHAII};*Pds*$^{+/+}$ mice, $n = 12$, *NS*). The effects of pendrin disruption on blood pressure remained limited, presumably because NCC is still markedly stimulated. Accordingly, no change in protein abundance of NCC and phosphor-T53 NCC was observed between Tg*Wnk4*^{PHAII};*Pds*$^{+/+}$ and Tg*Wnk4*^{PHAII};*Pds*$^{-/-}$ mice by immunoblot analyses of plasma membrane-enriched preparations isolated from renal cortex (Figure 7a). Protein abundance of ENaC subunits was also assessed. Both α and γ subunits decreased in Tg*Wnk4*^{PHAII};*Pds*$^{-/-}$ mice compared with Tg*Wnk4*^{PHAII};*Pds*$^{+/+}$ mice, consistent with the effect of isolated deletion of pendrin on ENaC expression described previously.[25]

We next measured total ENaC-dependent Na^+ absorption and K^+ secretion in double-mutant mice by assessing the effects of an acute injection of amiloride on urinary excretion of Na^+ and K^+. The natriuretic response to amiloride (Figure 7b, left panel) was not different between Tg*Wnk4*^{PHAII};*Pds*$^{+/+}$ and Tg*Wnk4*^{PHAII};*Pds*$^{-/-}$ mice, indicating that ENaC activity is not altered by pendrin disruption. However, the decrease in urinary K^+ excretion following amiloride was higher in Tg*Wnk4*^{PHAII};*Pds*$^{-/-}$ mice than in Tg*Wnk4*^{PHAII};*Pds*$^{+/+}$ mice (Figure 7b, right panel), suggesting that ENaC-dependent K^+ secretion is increased after pendrin disruption in Tg*Wnk4*^{PHAII} mice.

Table 1 | Blood parameters of control, Tg*Wnk4*^{PHAII};*Pds*$^{+/+}$, and Tg*Wnk4*^{PHAII};*Pds*$^{-/-}$ mice

Blood	Control	*TgWnk4*^{PHA2};*Pds*$^{+/+}$	*TgWnk4*^{PHA2};*Pds*$^{-/-}$
pH	7.26 ± 0.01	7.26 ± 0.01	7.30 ± 0.01$^{\#\#}$
PCO_2	56 ± 1	51 ± 1*	54 ± 2
HCO_3^-, mM	22.9 ± 0.7	20.8 ± 0.3*	23.7 ± 0.6$^{\#\#\#\#}$
Na^+, mM	148.5 ± 1.0	148.6 ± 0.6	149.9 ± 0.4
Cl^-, mM	109.1 ± 0.4	114.0 ± 0.4****	112.0 ± 0.5$^{\#\#}$
K^+, mM	4.40 ± 0.07	5.08 ± 0.08****	4.39 ± 0.06$^{\#\#\#\#}$
Hematocrit, %	42.5 ± 0.8	39.8 ± 0.4**	41.8 ± 0.5$^{\#\#}$

Cl^-, chloride ion; HCO_3^-, bicarbonate ion; K^+, potassium ion; Na^+, sodium ion; PCO_2, partial pressure of carbon dioxide.
Values are means ± SEM; N = 16, 39, and 29 for control, Tg*Wnk4*;*Pds*$^{+/+}$, and Tg*Wnk4*;*Pds*$^{-/-}$ mice, respectively. Statistical significance between groups was assessed by analysis of variance following Bonferroni's multiple comparison test when appropriate. Asterisks indicate statistical significance versus control mice (*$P < 0.05$, **$P < 0.01$, and ****$P < 0.0001$). The # symbols indicate statistical significance versus Tg*Wnk4*;*Pds*$^{+/+}$ mice (#$^{\#}P < 0.01$ and $^{\#\#\#\#}P < 0.0001$). No significant difference was observed between control and Tg*Wnk4*;*Pds*$^{-/-}$ mice.

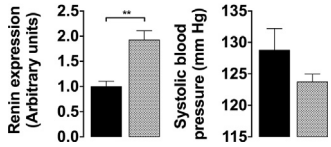

Figure 6 | Effect of pendrin deletion in Tg*Wnk4*^{PHAII} mice on renin expression and systolic blood pressure. Left panel: renin gene expression was analyzed by quantitative reverse-transcription polymerase chain reaction in whole kidney of 7 Tg*Wnk4*;*Pds*$^{+/+}$ (black bar) and 6 Tg*Wnk4*;*Pds*$^{-/-}$ (gray bar) mice. Results are expressed in arbitrary units relative to the expression of a geometrical mean of 4 housekeeping genes: ubiquitin, HPRT, 18s rRNA, and GAPDH. The Tg*Wnk4*;*Pds*$^{+/+}$ group has been arbitrarily set to 1. Values are represented as mean ± SEM. Statistical significance was assessed by unpaired Student *t*-test. **$P < 0.01$. Right panel: Systolic blood pressure was measured by telemetry in 6 Tg*Wnk4*;*Pds*$^{+/+}$ (black bar) and 5 Tg*Wnk4*;*Pds*$^{-/-}$ (gray bar) mice. Data correspond to the 12-hour night period mean ± SEM.

DISCUSSION

Studies performed either in humans or in animal models have confirmed that PHAII-causing mutations lead to increased phosphorylation, membrane expression, and activity of the cotransporter NCC of the DCT cells.

β-ICs exchange HCO_3^- for Cl^- through the apical Cl^-/HCO_3^- exchanger pendrin/SLC26A4, fulfilling their primary function of HCO_3^- excretion. When pendrin is functionally coupled with the Na^+-driven $Cl^-/2HCO_3^-$ exchanger NDCBE/SLC4A8, thiazide-sensitive, electroneutral NaCl absorption then occurs in these cells.[17] We therefore performed this study to determine to what extent pendrin might participate to the PHAII phenotype.

Here we show that pendrin activity and thiazide-sensitive electroneutral NaCl absorption through the pendrin/NDCBE transport system are activated in isolated CCDs of Tg*Wnk4*^{PHAII} mice. Elucidating the mechanism of pendrin activation was beyond the scope of this study. However, several studies in the literature support the idea that WNK4 is involved in pendrin activation. For instance, the pendrin/NDCBE transport system is the dominant mechanism accounting for Na^+ absorption in the CCD of *Ncc* knockout mice,[17] whereas in *Wnk4* knockout mice, which exhibit dramatically low NCC expression, Na^+ absorption in CCDs does not occur through the pendrin/NDCBE system but through ENaC.[11] Shibata *et al.* identified a phosphorylation site at S843 in the mineralocorticoid receptor ($MR^{S843\text{-}P}$) exclusively in ICs, which prevents ligand binding.[16] $MR^{S843\text{-}P}$ dephosphorylation restores MR activation by aldosterone and increases pendrin expression. Tg*Wnk4*^{PHAII} mice (gain of function of WNK4) have lower levels of $MR^{S843\text{-}P}$, whereas *Wnk4* knockout mice showed increased levels of $MR^{S843\text{-}P}$. Altogether, these studies strongly support the role of WNK4 in pendrin regulation through the modulation of MR phosphorylation.

Pendrin deletion in Tg*Wnk4*^{PHAII} mice decreases signs of hypervolemia. Renin expression and hematocrit were

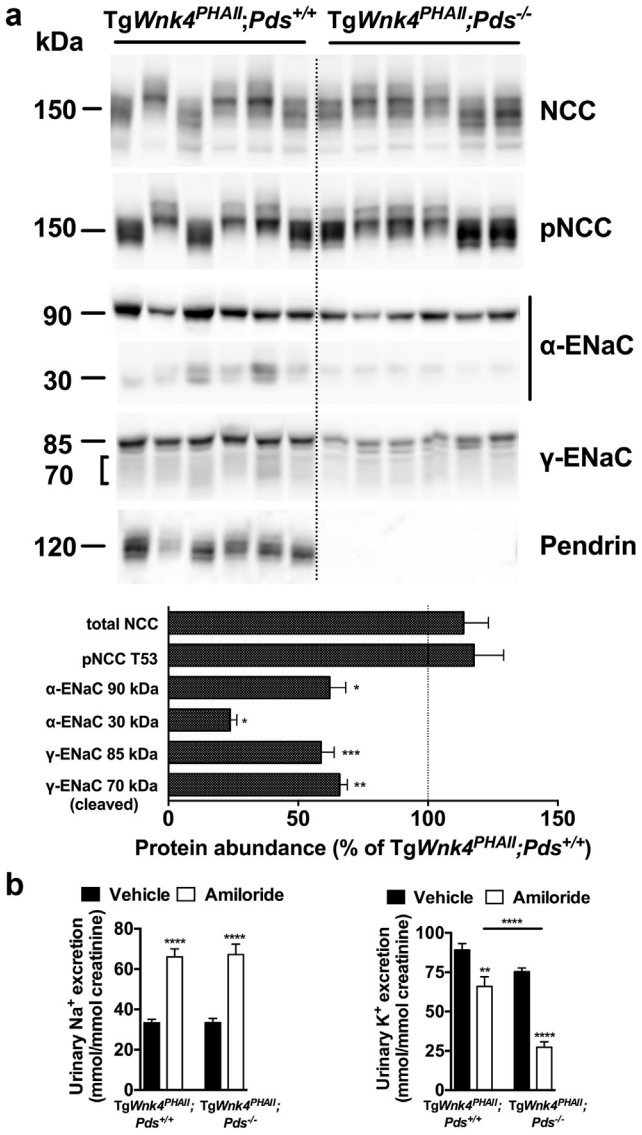

Figure 7 | Effect of pendrin deletion in Tg*Wnk4*^{PHAII} mice on sodium ion (Na^+) and chloride ion (Cl^-) transporters. (**a**) Immunoblots performed on plasma membrane-enriched fraction of renal cortex from Tg*Wnk4;Pds*$^{+/+}$ ($N = 6$) and Tg*Wnk4;Pds*$^{-/-}$ ($N = 6$) mice. Bar graph shows a summary of densitometric analyses. Densitometric values were normalized to the mean for the Tg*Wnk4;Pds*$^{+/+}$ mice that was defined as 100%, and results were expressed as mean ± SEM. Statistical significance was assessed by unpaired Student *t*-test. (**b**) Effect of amiloride injection on urinary Na^+ and potassium ion (K^+) excretion in Tg*Wnk4;Pds*$^{+/+}$ ($N = 7$) and Tg*Wnk4;Pds*$^{-/-}$ ($N = 5$) mice. Amiloride elicits significant increase in Na^+ excretion and decrease in K^+ excretion in both Tg*Wnk4;Pds*$^{+/+}$ and Tg*Wnk4;Pds*$^{-/-}$ mice 6 hours after injection. Amiloride induced natriuresis was not different between groups. K^+ excretion after amiloride was significantly lower in Tg*Wnk4;Pds*$^{-/-}$ mice, indicating that epithelial sodium channel (ENaC)-dependent K^+ secretion is increased in these mice. Values are the mean ± SEM. Statistical significance was assessed by 1-way analysis of variance. $^{**}P < 0.01$ and $^{****}P < 0.0001$, vehicle versus amiloride. $^{****}P < 0.0001$, Tg*Wnk4;Pds*$^{+/+}$ versus Tg*Wnk4;Pds*$^{-/-}$ mice following amiloride injection. To optimize viewing of this image, please see the online version of this article at www.kidney-international.org.

significantly increased in pendrin-deleted Tg*Wnk4*^{PHAII} mice compared with Tg*Wnk4*^{PHAII} mice, although not to the levels seen in control mice. There was a trend of decreasing systolic blood pressure in pendrin deleted Tg*Wnk4*^{PHAII} mice compared with Tg*Wnk4*^{PHAII} mice, but the difference (5 mm Hg) did not reach statistical significance, possibly because of the small number of mice per group. It is worth noting that, in the study by Lalioti *et al.*, the increase in systolic blood pressure in Tg*Wnk4*^{PHAII} mice compared with wild-type mice was about the same magnitude at 7 mm Hg.[8] Nevertheless, these results indicate that NCC hyperactivation is sufficient to drive hypertension in PHAII. As with NCC,[8] genetic deletion of pendrin in PHAII mice normalized blood K^+ concentration. Interestingly, overexpression of either NCC or pendrin has no effect on blood K^+ concentration.[12,18] Thus, concomitant activation of NCC and pendrin is necessary to drive hyperkalemia in this model. Conversely, combined deletion of NCC and NDCBE, the partner of pendrin in ICs, induces hypokalemia,[22] while isolated deletion of either NCC or pendrin in the mouse has no or slight effect on blood K^+ concentration under standard conditions.[19,20,26,27] These findings indicate that NCC and pendrin act in concert to control plasma K^+ concentration. Consistently, several studies have demonstrated that NCC is regulated by K intake and/or plasma K^+ level, with low K intake or hypokalemia activating NCC and high K intake inhibiting NCC.[28–30] Decreased plasma K^+ concentration was also shown to promote pendrin induction by aldosterone, a mechanism that has been proposed to counteract the progression of hypokalemia.[31] Our study suggests that these 2 mechanisms of protection against hypokalemia become aberrantly activated in PHAII mice and thereby participate in the generation of hyperkalemia. Increased activity of both NCC and the pendrin/NDCBE system is expected to favor the electroneutral NaCl reabsorption in the distal nephron at the expense of the electrogenic Na^+/K^+ exchange promoted by ENaC, therefore leading to K^+ retention.

We found that ENaC-dependent K^+ secretion was decreased in Tg*Wnk4*^{PHAII} mice and restored when pendrin was deleted. However, we were not able to detect any change in amiloride-induced urinary Na^+ excretion (reflecting total ENaC activity) between control, Tg*Wnk4*^{PHAII}, and pendrin-deleted Tg*Wnk4*^{PHAII} mice. Expected changes in ENaC protein expression were nevertheless observed between these mice. This suggests that ENaC activity is modulated by other factors such as HCO_3^- or ATP as previously demonstrated.[25,32] Altogether, these findings indicate that a decrease in K^+ channel activity *per se* is involved in the pathogenesis of hyperkalemia in this model. A decrease in renal outer medullary potassium channel (ROMK) expression in the DCT2/CNT was previously reported in a PHAII mouse model caused by a WNK1 mutation.[10]

A recent study by Grimm *et al.* proposed that tubular remodeling in response to NCC activation explains renal potassium retention in PHAII.[33] In this latter study, the authors showed that constitutive activation of STE20/SPS1-related proline/alanine-rich kinase in the DCT (CA-SPAK), which leads to PHAII phenotype, induces a marked increase in DCT1 mass, with a commensurate reduction in the CNT mass resulting in a dramatic decrease in both ENaC and ROMK expression. This latter model significantly differs from the one studied here. We observed an increase in CCD mass that is paralleled by an increase in pendrin activity with only a modest decrease in CNT mass (CNT fractional volumes were 5.16% ± 0.54% vs. 3.41% ± 0.36% of kidney cortex in control and Tg*Wnk4*^{PHAII} mice, respectively ($n = 4$ for each group, $P = 0.036$), which likely explains the decrease in ENaC and ROMK currents seen in the DCT2/early CNT of Tg*Wnk4*^{PHAII} mice.[34] However, the observation that pendrin deletion normalized blood K^+ concentration in Tg*Wnk4*^{PHAII} mice indicates that remodeling of the CNT is not the primary cause of K^+ retention in our model. In summary, both models (CA-SPAK and WNK4-PHAII) are characterized by the combination of NCC activation along with a second mechanism that differs from a model to another but that results ultimately in a decrease in K^+ secretion.

In vitro studies have shown direct inhibitory effect of WNK4 on ROMK or BK.[5,35] However, because decreased urinary K^+ secretion in Tg*Wnk4*^{PHAII} mice is reversed by pendrin deletion, it is unlikely that hyperkalemia in PHAII is the consequence of direct inhibition of ROMK and/or BK by WNK4. Changes in acid-base status affect potassium secretion in the distal nephron; specifically, metabolic acidosis inhibits whereas metabolic alkalosis stimulates K^+ secretion.[36] Consistent with this observation, it has been demonstrated that intracellular pH is an important modulator of the native low-conductance K^+ channel in CCD,[37,38] such that acidification within the physiological range results in a reduction of single channel activity. Thus, correction of the acidosis following pendrin deletion would remove the acidic pH inhibition of ROMK activity. The reversion of hyperkalemia by genetic ablation of pendrin in Tg*Wnk4*^{PHAII} mice could also be due to enhanced BK activity in ICs. The BKβ4 subunit is present with the BKα subunit in ICs as well as L-WNK1, which activates BK.[39] Chloride binding to WNK1 precludes its autophosphorylation and thereby inhibits kinase activity.[40] It is thus possible that inactivation of pendrin by decreasing intracellular Cl^- concentration activates L-WNK1 selectively in ICs, which in turns activates BK.

Finally, one of the most exciting findings is the identification of pendrin hyperactivity as a novel mechanism for renal acidosis. Indeed, our experiments shown in Figures 4 and 5 clearly demonstrated that the metabolic acidosis is not caused primarily by hyperkalemia or by defective V-ATPase activity. Indeed, (i) metabolic acidosis was not significantly alleviated by the normalization of blood K^+ concentration; and (ii) ammonium excretion and proton secretion were not impaired, and the mice were still able to achieve maximal urine acidification and ammonium excretion under stimulated condition. By contrast, our results showing that pendrin-mediated Cl^-/HCO_3^- exchange per cell as well as the total number of pendrin-expressing cells are markedly increased while pendrin genetic ablation completely corrects metabolic acidosis in Tg*Wnk4*^{PHAII} mice indicate that metabolic acidosis is caused by excessive bicarbonate secretion by the distal nephron.

Activation of pendrin in Tg*Wnk4*^{PHAII} mice is accompanied by an alteration of the structure of the CCD. Indeed, we show an increase in β-ICs at the expense of α-ICs in the CCDs of Tg*Wnk4*^{PHAII} mice. Several studies report that acidosis provokes the differentiation of α-ICs from β-ICs, but only one other study, by Grimm *et al.*, observes that the IC conversion works in the opposite direction in a *Spak* knockout mouse model,[41] which has very low level of NCC.[42] An increased number of pendrin-positive IC cells was also observed in *Ncc* knockout mice as the result of hyperplasia of the CNT seen in these mice.[43,44]

It might be puzzling, if metabolic acidosis is caused by a distal renal leak of bicarbonate, that Tg*Wnk4*^{PHAII} did not exhibit overt bicarbonaturia. However, this is also the case in patients with proximal renal acidosis when they are in steady state—that is, when they have overt metabolic acidosis due to compensatory mechanisms.[45–48] If not, these patients would not be in steady state and would die from uncontrolled acidosis. Generally, the renal leak of bicarbonate can be unmasked when blood bicarbonate concentration is normalized after massive infusion of bicarbonate. However, we were not able to perform this experiment in our model as the mice tolerated bicarbonate infusion very poorly and died during the bicarbonate infusion.

Interestingly, our observation might not be limited to PHAII patients. Indeed, it has been recently demonstrated that calcineurin inhibitors, which are extensively used as immunosuppressive agents in organ transplantation, alter the WNK signaling pathway, and thereby can activate NCC causing hypertension.[49] These patients do not only exhibit hypertension but are also frequently affected by hyperkalemia and metabolic acidosis.[50,51] It is tempting to speculate that pendrin hyperactivity will be also detected in these patients and can account for these symptoms.

In conclusion, our study demonstrates a role of pendrin in acid-base and potassium homeostasis, and identifies a renal leak of bicarbonate by the distal nephron as a novel type of renal tubular acidosis. We propose to define this novel mechanism of renal acidosis as type 5 RTA. It appears to be encountered also as side effects of the use of some calcineurin inhibitors.[49–51]

METHODS

Animal generation

Tg*Wnk4*^{PHAII} mice[8] were provided by Richard P. Lifton (Yale university, New Haven, CT). *Pds*$^{-/-}$ mice[52] were provided by Andrew Griffith (NIDCD, NIH, Rockville, MD). Tg*Wnk4*^{PHAII} animals, carrying 2 copies of the mutated WNK4 transgene, were bred with *Pds*$^{-/-}$ animals to generate double-heterozygote animals. Those were then bred

with Tg*Wnk4*^{PHAII} animals in order to obtain *Pds*$^{+/-}$ animals with 2 copies of the mutated Wnk4 transgene. Tg*Wnk4*^{PHAII};*Pds*$^{+/-}$ were then intercrossed to generate Tg*Wnk4*^{PHAII};*Pds*$^{+/+}$ and Tg*Wnk4*^{PHAII};*Pds*$^{-/-}$. In parallel, *Pds*$^{-/-}$ animals were crossed with C57Bl/6J mice over 2 generations in order to generate *Pds*$^{+/-}$ animals on the same mixed genetic background than the double-mutant mice, as *TgWnk4*^{PHAII} animals are from a C57Bl/6J background. The resulting *Pds*$^{+/-}$ mice were intercrossed to obtain *Pds*$^{+/+}$ (control) and *Pds*$^{-/-}$ mice.

Physiological studies

All experiments were conducted using male mice (3–5 months old) and performed in accordance with the relevant guidelines of the French Ministry of Agriculture (Authorization Executive Order B751532) for scientific experimentation on animals, the European Communities Council Directive, and international ethical standards.

For urine collection, individual mice were studied in metabolic cages (Tecniplast France, Lyon, France). Mice were pair-fed with standard laboratory powdered chow containing 0.3% sodium (INRA, Jouy-en-Josas, France). After 3 to 5 days of adjustment, 24-hour urine was collected under mineral oil.

Blood was sampled from the retro-orbital sinus of isofluorane-anesthetized mice.

Blood parameters and urinary analyses

Blood analyses were performed on an ABL 77 pH/Blood-Gas Analyzer (Radiometer, Copenhagen, Denmark). Blood bicarbonate concentration was calculated from the measured values using the Henderson-Hasselbach equation. Urinary Na^+ and K^+ electrolytes were measured with a flame photometer (IL943; Instruments Laboratory, Lexington, MA). Urinary pH was measured with a pH/blood-gas analyzer (ABL 555, Radiometer). Urinary NH_4^+ and titratable acid were measured by titration with a DL 55 titrator (Mettler Toledo, Viroflay, France). Urine aldosterone was measured by RIA (DPC Dade Behring/Siemens Healthcare, Erlangen, Germany). All urinary values were adjusted by urinary creatinine previously quantified by Jaffé colorimetric method.

Measurements of blood pressure by radiotelemetry

The catheter of the telemeter was inserted into the left femoral artery. The transmitter probe was positioned subcutaneously on the flank. After a 1-week recovery period in individual cages, mice were placed on a receiver and blood pressure (BP) and locomotor activity were recorded continuously in freely moving mice, in a light/dark-cycled recording room (7 a.m. to 7 p.m.), for 3 consecutive days on a normal diet as previously described.[21]

In vitro microperfusion of CCDs

CCDs were isolated and microperfused *in vitro* as previously reported.[17,18,32,53]

Immunofluorescence studies and immunoblot analyses

Kidneys were fixed *in situ* by retrograde perfusion of the aorta with a solution of 4% PFA in phosphate buffer. Harvested kidneys were washed in ice-cold phosphate buffer for 30 minutes before freezing in cold isopentane. Then 4-μm cryosections were stained with primary antibodies (a rabbit anti-pendrin diluted 1:200, a guinea pig anti-AE1 diluted 1:5,000, and a chicken anti-Atp6v1e1, which detects the V-ATPase, diluted 1:500), and secondary antibodies (goat anti-rabbit Alexa 555 diluted 1/800 (Invitrogen, Carlsbad, CA), donkey anti–guinea pig Cy5 diluted 1:2,000 (Jackson ImmunoResearch Laboratories, West Grove, PA), goat anti-chicken Alexa 488 diluted 1/2000 (Invitrogen). Images were acquired with a Zeiss LSM 710 laser scanning microscope (Carl Zeiss France, Marly-le-Roi, France). Fractional volume of CCDs was measured as described previously.[54] For Western blot analyses, 15 μg of the plasma membrane-enriched protein fraction isolated from renal cortex was separated on reducing 7.5% or 10% SDS-polyacrylamide gels. Protein loading was assessed on gels run in parallel and stained with Coomassie blue.[55] Blots were probed with anti-NCC, 1:10,000; anti-NCC phospho-Thr53; 1:10,000; anti-α-ENaC, 1:5,000; anti-γ-ENaC, 1:10,000; and anti-pendrin, 1:3,000. For a complete description of all the study methods, see the Supplementary Methods.

DISCLOSURE

All the authors declared no competing interests.

ACKNOWLEDGMENTS

We thank Nikita Radionov and Bettina Serbin for technical assistance. RC and DE are funded by INSERM, CNRS, and grants from l'Agence Nationale de la Recherche (ANR BLANC 2012-R13011KK to RC and ANR BLANC 14-CE12-0013-01/ HYPERSCREEN to DE). DE is also funded by a CHLORBLOCK grant from the IDEX Sorbonne Paris Cité and an ECOS/CONICYT France-Chile 2014 grant. MJ is funded by the CODDIM from the Région Ile de France. KIL received a fellowship from the CONICYT. FT was funded by ERA-EDTA LTF 141-2013. MC was funded by collaborative funding from the Consejo Nacional de Ciencia y Tecnología and ANR (Conacyt 188712 - ANR 12-ISVS1-0001-01). CB was funded by the Lefoulon-Delalande Fundation.

SUPPLEMENTARY MATERIAL

Supplementary Methods.

Figure S1. Response of *Wnk1*$^{+/FHHt}$ mice to an acid load. Blood pH, pCO2, Cl^-, and HCO_3^- were measured in *Wnk1*$^{+/FHHt}$ mice and in control mice (*Wnk1*$^{+/i1lox}$) in basal conditions and after administrating 280 mM of NH_4Cl in drinking water for 7 days. Urine pH and urinary NH_4^+ were also measured at basal conditions (day 0) and at days 2 and 7. Values of blood and urinary parameters are represented as the mean ± SEM. Statistical significance is assessed by 1-way analysis of variance ($n = 8$ per group, $^*P < 0.05$, $^{**}P < 0.01$, $^{***}P < 0.001$).

Supplementary material is linked to the online version of the paper at www.kidney-international.org.

REFERENCES

1. Gordon RD. Syndrome of hypertension and hyperkalemia with normal glomerular filtration rate. *Hypertension*. 1986;8:93–102.
2. Schambelan M, Sebastian A, Rector FC Jr. Mineralocorticoid-resistant renal hyperkalemia without salt wasting (type II pseudohypoaldosteronism): role of increased renal chloride reabsorption. *Kidney Int*. 1981;19:716–727.
3. Wilson FH, Disse-Nicodeme S, Choate KA, et al. Human hypertension caused by mutations in WNK kinases. *Science*. 2001;293:1107–1112.
4. Hadchouel J, Ellison DH, Gamba G. Regulation of renal electrolyte transport by WNK and SPAK-OSR1 kinases. *Annu Rev Physiol*. 2016;78:367–389.
5. Kahle KT, Wilson FH, Leng Q, et al. WNK4 regulates the balance between renal NaCl reabsorption and K+ secretion. *Nat Genet*. 2003;35:372–376.
6. Boyden LM, Choi M, Choate KA, et al. Mutations in kelch-like 3 and cullin 3 cause hypertension and electrolyte abnormalities. *Nature*. 2012;482:98–102.
7. Louis-Dit-Picard H, Barc J, Trujillano D, et al. KLHL3 mutations cause familial hyperkalemic hypertension by impairing ion transport in the distal nephron. *Nat Genet*. 2012;44:456–460. S451–S453.
8. Lalioti MD, Zhang J, Volkman HM, et al. Wnk4 controls blood pressure and potassium homeostasis via regulation of mass and activity of the distal convoluted tubule. *Nat Genet*. 2006;38:1124–1132.

9. Yang SS, Morimoto T, Rai T, et al. Molecular pathogenesis of pseudohypoaldosteronism type II: generation and analysis of a Wnk4(D561A/+) knockin mouse model. *Cell Metab*. 2007;5:331–344.
10. Vidal-Petiot E, Elvira-Matelot E, Mutig K, et al. WNK1-related Familial Hyperkalemic Hypertension results from an increased expression of L-WNK1 specifically in the distal nephron. *Proc Natl Acad Sci U S A*. 2013;110:14366–14371.
11. Castaneda-Bueno M, Cervantes-Perez LG, Vazquez N, et al. Activation of the renal Na+:Cl- cotransporter by angiotensin II is a WNK4-dependent process. *Proc Natl Acad Sci U S A*. 2012;109:7929–7934.
12. McCormick JA, Nelson JH, Yang CL, et al. Overexpression of the sodium chloride cotransporter is not sufficient to cause familial hyperkalemic hypertension. *Hypertension*. 2011;58:888–894.
13. Hadchouel J, Soukaseum C, Busst C, et al. Decreased ENaC expression compensates the increased NCC activity following inactivation of the kidney-specific isoform of WNK1 and prevents hypertension. *Proc Natl Acad Sci U S A*. 2010;107:18109–18114.
14. Ronzaud C, Loffing-Cueni D, Hausel P, et al. Renal tubular NEDD4-2 deficiency causes NCC-mediated salt-dependent hypertension. *J Clin Invest*. 2013;123:657–665.
15. Ohno M, Uchida K, Ohashi T, et al. Immunolocalization of WNK4 in mouse kidney. *Histochem Cell Biol*. 2011;136:25–35.
16. Shibata S, Rinehart J, Zhang J, et al. Mineralocorticoid receptor phosphorylation regulates ligand binding and renal response to volume depletion and hyperkalemia. *Cell Metab*. 2013;18:660–671.
17. Leviel F, Hubner CA, Houillier P, et al. The Na+-dependent chloride-bicarbonate exchanger SLC4A8 mediates an electroneutral Na+ reabsorption process in the renal cortical collecting ducts of mice. *J Clin Invest*. 2010;120:1627–1635.
18. Jacques T, Picard N, Miller RL, et al. Overexpression of pendrin in intercalated cells produces chloride-sensitive hypertension. *J Am Soc Nephrol*. 2013;24:1104–1113.
19. Verlander JW, Hassell KA, Royaux IE, et al. Deoxycorticosterone upregulates PDS (Slc26a4) in mouse kidney: role of pendrin in mineralocorticoid-induced hypertension. *Hypertension*. 2003;42:356–362.
20. Wall SM, Kim YH, Stanley L, et al. NaCl restriction upregulates renal Slc26a4 through subcellular redistribution: role in Cl- conservation. *Hypertension*. 2004;44:982–987.
21. Trepiccione F, Soukaseum C, Baudrie V, et al. Acute genetic ablation of pendrin lowers blood pressure in mice. *Nephrol Dial Transplant*. 2017;32:1137–1145.
22. Sinning A, Radionov N, Trepiccione F, et al. Double knockout of the Na+-driven Cl-/HCO3- exchanger and Na+/Cl- cotransporter induces hypokalemia and volume depletion. *J Am Soc Nephrol*. 2017;28:130–139.
23. DuBose TD Jr. Hyperkalemic hyperchloremic metabolic acidosis: pathophysiologic insights. *Kidney Int*. 1997;51:591–602.
24. Schwartz GJ, Barasch J, Al-Awqati Q. Plasticity of functional epithelial polarity. *Nature*. 1985;318:368–371.
25. Kim YH, Pech V, Spencer KB, et al. Reduced ENaC protein abundance contributes to the lower blood pressure observed in pendrin-null mice. *Am J Physiol Renal Physiol*. 2007;293:F1314–F1324.
26. Schultheis PJ, Lorenz JN, Meneton P, et al. Phenotype resembling Gitelman's syndrome in mice lacking the apical Na+-Cl- cotransporter of the distal convoluted tubule. *J Biol Chem*. 1998;273:29150–29155.
27. Amlal H, Petrovic S, Xu J, et al. Deletion of the anion exchanger Slc26a4 (pendrin) decreases apical Cl(-)/HCO3(-) exchanger activity and impairs bicarbonate secretion in kidney collecting duct. *Am J Physiol Cell Physiol*. 2010;299:C33–C41.
28. Zhang C, Wang L, Zhang J, et al. KCNJ10 determines the expression of the apical Na-Cl cotransporter (NCC) in the early distal convoluted tubule (DCT1). *Proc Natl Acad Sci U S A*. 2014;111:11864–11869.
29. Terker AS, Zhang C, McCormick JA, et al. Potassium modulates electrolyte balance and blood pressure through effects on distal cell voltage and chloride. *Cell Metab*. 2015;21:39–50.
30. Wang MX, Cuevas CA, Su XT, et al. Potassium intake modulates the thiazide-sensitive sodium-chloride cotransporter (NCC) activity via the Kir4.1 potassium channel. *Kidney Int*. 2018;93:893–902.
31. Xu N, Hirohama D, Ishizawa K, et al. Hypokalemia and pendrin induction by aldosterone. *Hypertension*. 2017;69:855–862.
32. Gueutin V, Vallet M, Jayat M, et al. Renal beta-intercalated cells maintain body fluid and electrolyte balance. *J Clin Invest*. 2013;123:4219–4231.
33. Grimm PR, Coleman R, Delpire E, et al. Constitutively active SPAK causes hyperkalemia by activating NCC and remodeling distal tubules. *J Am Soc Nephrol*. 2017;28:2597–2606.
34. Zhang C, Wang L, Su XT, et al. ENaC and ROMK activity are inhibited in the DCT2/CNT of TgWnk4PHAII mice. *Am J Physiol Renal Physiol*. 2017;312:F682–F688.
35. Zhuang J, Zhang X, Wang D, et al. WNK4 kinase inhibits Maxi K channel activity by a kinase-dependent mechanism. *Am J Physiol Renal Physiol*. 2011;301:F410–F419.
36. Aronson PS, Giebisch G. Effects of pH on potassium: new explanations for old observations. *J Am Soc Nephrol*. 2011;22:1981–1989.
37. Wang WH, Schwab A, Giebisch G. Regulation of small-conductance K+ channel in apical membrane of rat cortical collecting tubule. *Am J Physiol*. 1990;259:F494–F502.
38. Wang WH. Regulation of the hyperpolarization-activated K+ channel in the lateral membrane of the cortical collecting duct. *J Gen Physiol*. 1995;106:25–43.
39. Liu Y, Song X, Shi Y, et al. WNK1 activates large-conductance Ca2+-activated K+ channels through modulation of ERK1/2 signaling. *J Am Soc Nephrol*. 2015;26:844–854.
40. Piala AT, Moon TM, Akella R, et al. Chloride sensing by WNK1 involves inhibition of autophosphorylation. *Sci Signal*. 2014;7:ra41.
41. Grimm PR, Lazo-Fernandez Y, Delpire E, et al. Integrated compensatory network is activated in the absence of NCC phosphorylation. *J Clin Invest*. 2015;125:2136–2150.
42. McCormick JA, Mutig K, Nelson JH, et al. A SPAK isoform switch modulates renal salt transport and blood pressure. *Cell Metab*. 2011;14:352–364.
43. Loffing J, Vallon V, Loffing-Cueni D, et al. Altered renal distal tubule structure and renal Na(+) and Ca(2+) handling in a mouse model for Gitelman's syndrome. *J Am Soc Nephrol*. 2004;15:2276–2288.
44. Vallet M, Picard N, Loffing-Cueni D, et al. Pendrin regulation in mouse kidney primarily is chloride-dependent. *J Am Soc Nephrol*. 2006;17:2153–2163.
45. Rodriguez Soriano J, Boichis H, Stark H, et al. Proximal renal tubular acidosis. A defect in bicarbonate reabsorption with normal urinary acidification. *Pediatr Res*. 1967;1:81–98.
46. Rodriguez Soriano J. Renal tubular acidosis: the clinical entity. *J Am Soc Nephrol*. 2002;13:2160–2170.
47. Haque SK, Ariceta G, Batlle D. Proximal renal tubular acidosis: a not so rare disorder of multiple etiologies. *Nephrol Dial Transplant*. 2012;27:4273–4287.
48. Soriano JR, Boichis H, Edelmann CM Jr. Bicarbonate reabsorption and hydrogen ion excretion in children with renal tubular acidosis. *J Pediatr*. 1967;71:802–813.
49. Hoorn EJ, Walsh SB, McCormick JA, et al. The calcineurin inhibitor tacrolimus activates the renal sodium chloride cotransporter to cause hypertension. *Nat Med*. 2011;17:1304–1309.
50. Tanrisev M, Gungor O, Kocyigit I, et al. Renal tubular acidosis in renal transplant patients: the effect of immunosuppressive drugs. *Ann Transplant*. 2015;20:85–91.
51. Keven K, Ozturk R, Sengul S, et al. Renal tubular acidosis after kidney transplantation–incidence, risk factors and clinical implications. *Nephrol Dial Transplant*. 2007;22:906–910.
52. Everett LA, Belyantseva IA, Noben-Trauth K, et al. Targeted disruption of mouse Pds provides insight about the inner-ear defects encountered in Pendred syndrome. *Hum Mol Genet*. 2001;10:153–161.
53. Chambrey R, Kurth I, Peti-Peterdi J, et al. Renal intercalated cells are rather energized by a proton than a sodium pump. *Proc Natl Acad Sci U S A*. 2013;110:7928–7933.
54. Mutig K, Kahl T, Saritas T, et al. Activation of the bumetanide-sensitive Na+, K+,2Cl- cotransporter (NKCC2) is facilitated by Tamm-Horsfall protein in a chloride-sensitive manner. *J Biol Chem*. 2011;286:30200–30210.
55. Quentin F, Chambrey R, Trinh-Trang-Tan MM, et al. The Cl-/HCO3- exchanger pendrin in the rat kidney is regulated in response to chronic alterations in chloride balance. *Am J Physiol Renal Physiol*. 2004;287:F1179–F1188.